ORIGINAL ARTICLE

The Warsaw breakage syndrome-related protein DDX11 is required for ribosomal RNA synthesis and embryonic development

Xinliang Sun[1,2,†], Hongbo Chen[1,2,*,†], Zaian Deng[1,2], Bo Hu[3], Hui Luo[4], Xiaobin Zeng[4], Liqiao Han[5], Guoping Cai[1,2,*] and Lan Ma[1,2,*]

[1]School of Life Sciences, Tsinghua University, Beijing, China, [2]Division of Life Science and Health, Graduate School at Shenzhen, Tsinghua University, Shenzhen, China, [3]Department of Laboratory Medicine, The Third Affiliated Hospital of Sun Yat-sen University, Guangdong, China, [4]Department of Pharmacology, Guangdong Medical College, Zhanjiang 524023, Guangdong, China and and [5]Department of Laboratory Science, The Second Affiliated Hospital of Guangzhou University of Chinese Medicine, Guangdong, China

*To whom correspondence should be addressed at: Division of Life Science and Health, Graduate School at Shenzhen, Tsinghua University, Shenzhen, China. Tel: +86 75526033033; Fax: +86 75526033033; Email: malan@sz.tsinghua.edu.cn (L. M.); School of Life Sciences, Tsinghua University, Beijing, China. Email: caigp@mail.tsinghua.edu.cn (G. C.); Division of Life Science and Health, Graduate School at Shenzhen, Tsinghua University, Shenzhen, China. Tel: +86 75526035209; Fax: +86 75526035209; Email: chen.hongbo@sz.tsinghua.edu.cn (H. C.)

Abstract

DDX11 was recently identified as a cause of Warsaw breakage syndrome (WABS). However, the functional mechanism of DDX11 and the contribution of clinically described mutations to the pathogenesis of WABS are elusive. Here, we show that DDX11 is a novel nucleolar protein that preferentially binds to hypomethylated active ribosomal DNA (rDNA) gene loci, where it interacts with upstream binding factor (UBF) and the RNA polymerase I (Pol I). DDX11 knockdown changed the epigenetic state of rDNA loci from euchromatic structures to more heterochromatic structures, reduced the activity of UBF, decreased the recruitment of UBF and RPA194 (a subunit of Pol I) to rDNA promoter, suppressed rRNA transcription and thereby inhibited growth and proliferation of HeLa cells. Importantly, two indentified WABS-derived mutants, R263Q and K897del, and a Fe–S deletion construct demonstrated significantly reduced binding abilities to rDNA promoters and lowered DNA-dependent ATPase activities compared with wild-type DDX11. Knockdown of the zebrafish ortholog of human DDX11 by morpholinos resulted in growth retardation and vertebral and craniofacial malformations in zebrafish, concomitant with the changes in histone epigenetic modifications at rDNA loci, the reduction of Pol I recruitment to the rDNA promoter and a significant decrease in nascent pre-RNA levels. These growth disruptions in zebrafish in response to DDX11 reduction showed similarities to the clinically described developmental abnormalities found in WABS patients for the first time in any vertebrate. Thus, our results indicate that DDX11 functions as a positive regulator of rRNA transcription and provides a novel insight into the pathogenesis of WABS.

Introduction

Helicases are a class of enzymes that unwind annealed DNA, RNA or RNA–DNA hybrid duplexes using energy derived from ATP hydrolysis. These enzymes participate in varied cellular processes, including DNA replication, DNA repair, RNA transcription and RNA modification (1). All known helicases contain seven highly conserved motifs and are divided into six

superfamilies (2). Superfamily 2 (SF2) helicases containing an iron–sulfur (Fe–S) motif and a DEAD/DEAH-box have received considerable attention owing to their genetic links with human diseases (3–5). For example, patients who harbor mutations in the Xeroderma pigmentosum group D (XPD) and Fanconi anemia group J protein (FANCJ) helicases, two numbers of the SF2 superfamily, develop Cockayne's syndrome and Fanconi anemia, respectively (6,7). Recently, mutations in the DDX11 gene (also named Ch1R1), a newly discovered member of SF2 superfamily, were identified as a cause of Warsaw breakage syndrome (WABS), a newly defined recessive cohesinopathy. People diagnosed with WABS demonstrate congenital abnormalities, including severe pre- and postnatal growth retardation, facial dysmorphy, microcephaly and intellectual disabilities (8,9).

Recently, the functions of DDX11 have been extensively investigated. Similar to other DEAD (Asp–Glu–Ala–Asp)/DEAH (Asp–Glu–Ala–His) helicases, DDX11 protein possesses the capacity to unwind both DNA/DNA and DNA/RNA duplexes by hydrolyzing ATP in an *in vitro* system (9,10). The biochemical functions of two patient-derived mutations, K897del (a deletion of a single lysine in the extreme C terminus of ChlR1) and R263Q, were also extensively studied. The results showed that both these two mutations impaired the helicase activity of DDX11 on forked duplex or D-loop DNA substrates by perturbing the DNA binding and DNA-dependent ATPase activity. These findings provide us important insights into the clinical symptoms of WABS and biochemical functions associated with DDX11 mutations (9,10). In addition, the biological functions of DDX11 have also been investigated in several other contexts. The DDX11 homolog in yeast has been shown to play important roles in maintaining sister chromatin cohesion and regulating the G2/M cell cycle checkpoint (11). Subsequent studies have demonstrated that DDX11 deficiency also resulted in aneuploidy, cohesion defects, sister chromatid missegregation and increased apoptosis in mammalian cells (12–14). Consistent with these functions, DDX11 was shown to interact with the Ctf18–RFC complex (15), which is required for cohesion establishment. Further, DDX11-deficient cells were hypersensitive to DNA cross-linking agents or a topoisomerase I inhibitor, suggesting that DDX11 is important for DNA repair (16–18). Together, these results indicate that DDX11 maintains genomic stability by promoting proper sister chromatid cohesion and chromosome segregation in M phase. To examine the potential role of DDX11 during development, DDX11 knockout mice and mice with an ENU-induced mutation in the motif V domain of DDX11 were generated (14,19). However, these mice failed to thrive beyond embryonic stage, highlighting the requirement for DDX11 during mouse embryonic development.

Many proteins that play essential roles in normal cellular activities may also contribute aberrantly under conditions of pathogenesis. Previous work demonstrated that in addition to its localization to the condensed chromatin in the early stage of mitosis, the spindle poles throughout mitosis and the midbody during the later stages of mitosis (13), DDX11 also localizes to nucleoli in cells in interphase, which suggests that DDX11 might have unknown functions in the nucleolus. Functionally, the nucleolus is the site of ribosome biogenesis. Ribosome biogenesis is a multistage process that involves nascent 47S pre-rRNA transcription, rRNA processing into the mature 18S, 5.8S and 28S rRNAs, and ribosomal subunit assembly (20). During ribosome biogenesis, the rate-limiting step is rRNA transcription from rDNA loci, which are organized into tandem repeats within nucleolar organizer regions (21). This process is stringently regulated by diverse cellular signals and transcriptional regulatory factors, which are modified by growth factor stimulation,

nutrient availability or cellular stress. The rRNA transcription is mainly regulated at two levels: through control of the epigenetic states of rDNA loci and regulation of the activity of the transcriptional apparatus on the active rDNA loci (22–24). In mammalian cells, the epigenetic regulation of rDNA loci involves DNA methylation and histone modifications (25,26). Generally, CpG island hypomethylation and high levels of histone acetylation and H3K4 methylation are detected in the promoter regions of active rDNA loci; repressed promoters are associated with high levels of H3K9 methylation and CpG island hypermethylation (27,28). Several proteins have been suggested to regulate rDNA transcription by altering the epigenetic states of rDNA loci (27,29). In addition, the assembly of the polymerase I (Pol I) transcriptional apparatus at rDNA loci is necessary for rRNA transcription. Upstream binding factor (UBF) is a key transcriptional transactivator that binds to the upstream core element of rDNA loci and subsequently recruits SL1 and RNA Pol I to initiate rDNA transcription (21). Many studies have shown that the activity of UBF can be regulated by multiple post-translational modifications, including phosphorylation and acetylation (30,31). A growing body of work has demonstrated a strong link between dysregulation of ribosome biogenesis and various human diseases, in particular to mental disorders, anemia, developmental defects, aging and different types of cancer (32–34).

Here, we demonstrate that DDX11 is a novel nucleolus-localized protein that functions as a positive regulator for rRNA transcription, which preferentially binds to hypomethylated rDNA loci. DDX11 knockdown has been shown to induce epigenetic changes in rDNA loci and suppress the recruitment of UBF and RPA194 (a subunit of Pol I) to rDNA promoter regions. We also show that mutations in DDX11 identified in the genome of WABS patients functionally reduces the ability of DDX11 to bind to rDNA promoters and decreases their enzymatic activities, leading to reduced rRNA transcriptional rates. These results indicate that nucleolar dysfunction caused by DDX11 mutations may play a role in the pathogenesis of WABS. Consistent with these results *in vitro*, examination of zebrafish embryos with depleted levels of the zebrafish analog of DDX11 (zDDX11) also shows significantly decreased pre-rRNA levels compared with zebrafish in control groups. Importantly, knockdown of zDDX11 partially mimics the disease phenotypes observed in human WABS patients, which has not been observed in any other vertebrate models. Thus, our findings provide novel insights into the normal function of DDX11 as well as the underlying pathogenesis of WABS.

Results

DDX11 is a nucleolar protein

To assess potential functions of the DDX11 protein, we performed motif analysis using 'motif scan', an online tool (MyHits, SIB, Switzerland). The results of this analysis showed that DDX11 has a typical nuclear localization signal (NLS) sequence (aa295-312, Refseq no. NM_030653.3) and a glutamic-acid-rich region (aa163-224). To explore the subcellular distribution of endogenous DDX11 protein, we immunofluorescently labeled DDX11 using both mouse monoclonal and rabbit polyclonal antibodies in HeLa and HEK293 cells. As shown in Figure 1A and B, endogenous DDX11 had discrete globular aggregates in the nucleus, indicating that DDX11 is potentially a nucleolar protein. In addition, DDX11 co-localized with nucleolin protein, an established nucleolus marker, in the nucleus (Fig. 1C). Similar results were observed in HEK293 cells (data not shown). To confirm these results, HeLa cells were fractionated into cytoplasmic, nuclear
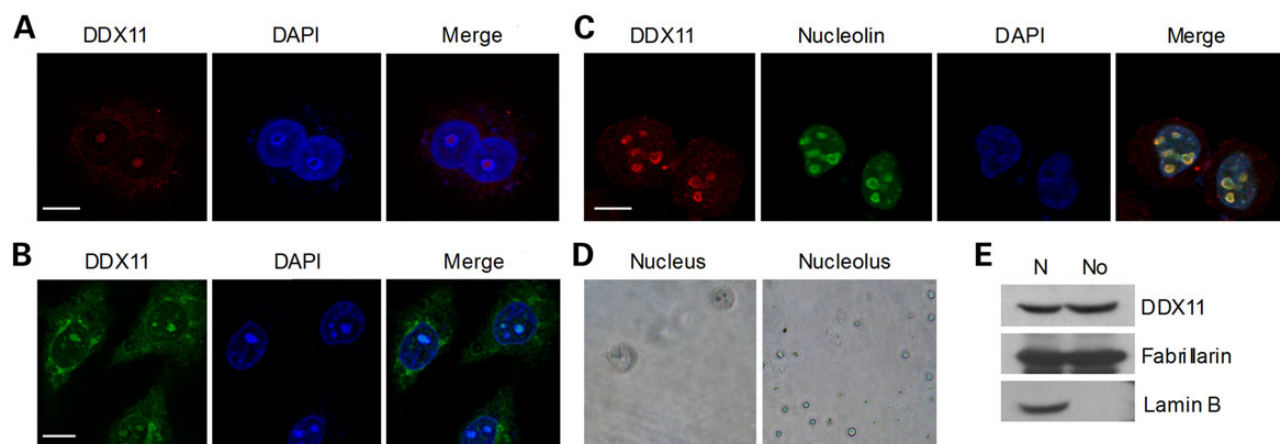
Figure 1. DDX11 is a nucleolar protein. (**A**) DDX11 was observed using confocal microscopy following treatment with a mouse primary antibody against DDX11 and a rhodamine-labeled goat anti-mouse secondary antibody in HeLa cells. Scale bar, 10 μm. (**B**) DDX11 was observed using confocal microscopy following treatment with a rabbit primary antibody against DDX11 and a FITC-labeled goat anti-rabbit secondary antibody. Scale bar, 10 μm. (**C**) DDX11 (red fluorescence) colocalizes with nucleolin (green fluorescence) in nucleoli. Scale bar, 10 μm. (**D**) HeLa cells were fractioned into nuclear (left image) and nucleolar (right image) fractions, and (**E**) the proteins were detected by western blotting using the indicated antibodies.

and nucleolar fractions (Fig. 1D), and protein extracts were analyzed using western blotting. Endogenous DDX11 protein was detected specifically in the nucleolar fraction (Fig. 1E). Together, these data suggest that the DDX11 protein contains typical NLSs and functions as a nucleolar protein.

DDX11 knockdown suppresses the transcription of rRNA genes, cell growth and proliferation

We next investigated the functional role of DDX11 in the nucleoli. The nucleolus is the site of rRNA synthesis and ribosome subunit assembly. The initial transcriptional product of the rDNA gene is the 47s pre-rRNA. The 5′-external transcribed spacer (5′-ETS) can be rapidly excised from 47S pre-rRNA by pre-rRNA processing proteins (Fig. 2A), so the 5′-ETS levels can be used to determine the transcriptional rate of the rDNA gene. HeLa or HEK293 cells were transfected with control or DDX11-specific siRNAs (Fig. 2B), and the amount of the nascent 47S pre-rRNA was quantified using qPCR. In HeLa cells, a marked decrease in 47S pre-rRNA levels was observed in cells transfected with DDX11-specific siRNAs compared with cells transfected with control siRNA (Fig. 2C), suggesting that knockdown of DDX11 protein suppressed the transcription of the rDNA gene. Similar results were observed in HEK293 cells (data not shown).

Luciferase reporter plasmids cloned with specific promoter sequences have been widely used to measure gene transcriptional activity. To further determine the effects of DDX11 on transcription of the rDNA gene, pHrD-IRES-Luc, a plasmid containing the human rRNA promoter and luciferase reporter, was co-transfected into HeLa cells together with control or DDX11-specific siRNAs, and luciferase activity was quantified using a luminometer at 48 h after transfection. As shown in Figure 2D, knockdown of DDX11 significantly inhibited the rRNA promoter-driven luciferase activity. Similar results were observed in HEK293 cells (data not shown).

In addition, the effects of DDX11 on rRNA transcription were further assessed using a fluorine-conjugated UTP analog (FUrd) incorporation assay. In cells transfected with control siRNA, we detected higher immunofluorescent signals at nucleolar sites. In contrast, cells transfected with DDX11 siRNA demonstrated a pronounced decrease in fluorescent intensity at nucleolar sites,

suggesting that DDX11 knockdown suppressed the nucleolar FUrd incorporation (Fig. 3A). Because ribosome biogenesis is prerequisite for cell growth and proliferation (35), we examined the effects of DDX1 siRNA on cellular growth. As expected, DDX11 knockdown also significantly inhibited cell growth and proliferation (Fig. 3B) and colony formation (Fig. 3C) compared with control cells.

Taken together, these data demonstrated that DDX11 plays an important role in regulating rRNA synthesis, cell growth and proliferation.

DDX11 associates with rDNA and Pol I transcriptional machinery

To further dissect the mechanism of DDX11's role in rRNA transcription, chromatin immunoprecipitation (ChIP) was performed using a DDX11 antibody in HeLa cells. Figure 4A depicts the positions of the sets of primers on the rDNA gene loci used for the ChIP assay. As shown in Figure 4B, DDX11 binding on the entire rDNA loci was enriched 2- to 8-fold compared with controls, suggesting that DDX11 participates in the regulation of rDNA transcription through direct binding to the rDNA loci.

rRNA transcription requires the recruitment of Pol I transcriptional machinery to rRNA loci. Pol I transcriptional machinery consists of at least three factors, UBF1, SL1 and RNA polymerase I. Several proteins have been shown to regulate the activity of Pol I transcriptional machinery through their interactions with these factors (36). To determine whether DDX11 is associated with Pol I transcriptional machinery, a co-immunoprecipitation assay was performed using an anti-DDX11 antibody, followed by detection of UBF and RPA194, a subunit of polymerase I, by western blotting. As shown in Figure 4C and D, DDX11 specifically interacted with UBF and RPA194, demonstrating that DDX11 associates with rDNA and Pol I transcriptional machinery.

DDX11 binds to active rDNA loci as a positive regulatory factor of rRNA transcription

Because we observed that DDX11 knockdown suppressed rRNA transcription, we hypothesized that DDX11 functions as a positive regulatory factor for rRNA synthesis. Previous studies have
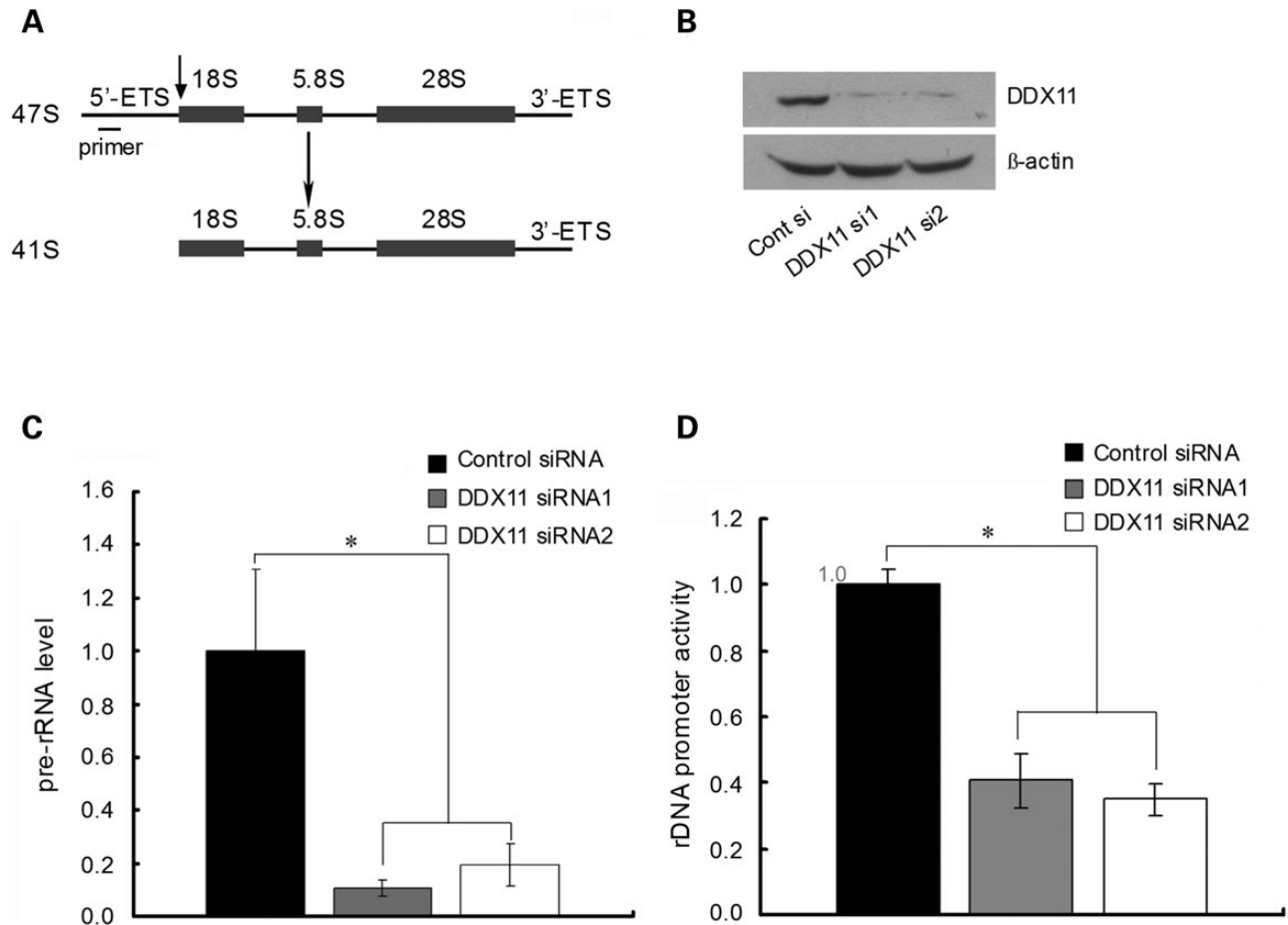
Figure 2. DDX11 is required for rRNA transcription. (**A**) The position of the primers on the 47S rRNA used for qPCR to detect nascent pre-rRNA levels. (**B**) HeLa cells were transfected with control or DDX11-specfic siRNAs. Cell lysates were prepared at 48 h post-transfection and DDX11 levels were analyzed by western blotting. (**C**) Control or DDX11-specific siRNAs were transfected into HeLa cells for 48 h, total RNA was extracted and qPCR was performed with primers shown in (A). The experiment was repeated three times, and results were presented as mean ± SD (*P < 0.05). (**D**) Control or DDX11-specific siRNAs were transfected into HeLa cells. The pHrD-IRES-Luc and pRL-TK plasmids were then co-transfected into the cells 24 h after siRNA transfection, and luciferase activity was measured 24 h later. Data from three independent experiments was presented as mean ± SD (*P < 0.05).

shown that growth factor stimulation can upregulate expression of proteins of the core transcriptional apparatus and other positive regulatory factors (37). In response to serum stimulation, expression levels of DDX11 markedly increased, concomitant with RPA194 and phosphorylated UBF (Ser388) in HeLa cells (Fig. 5A), suggesting that DDX11 is a positive regulatory factor of rRNA transcription.

Active rRNA loci have a euchromatic structure, characterized by relatively low levels of CpG island methylation, whereas inactive rRNA loci have a heterochromatic structure with higher levels of CpG island methylation (25). Studies have demonstrated that the positive transcriptional regulators specifically associate with hypomethylated active DNA (27–29). Because the expression levels of DDX11 increased upon serum stimulation, and knockdown of DDX11 correlated with reduced levels of 47S pre-rRNA, we hypothesized that as a positive regulator of rRNA transcription, DDX11 might preferentially bind to active rDNA loci. In order to examine this hypothesis, we utilized the ChIP-chop assay in HeLa cells. Specifically, chromatin fragments from an input sample or ChIP samples against DDX11, UBF and RPA194 antibodies were digested with the methylation-sensitive enzyme, HpaII, and then qPCR was performed using primer pairs flanking an HpaII site within the rDNA promoter region. As

shown in Figure 5B, chromatin fragments immunoprecipitated with DDX11 showed a similar level of HpaII-resistance (normalized to the mock digestion) to that of UBF and RPA194, which was lower than that of input DNA. UBF and RPA194 have previously been shown to be positive regulatory factors for rDNA transcription and are predominantly found at active rDNA loci. These results suggest that DDX11 is also a positive regulatory factor that predominantly binds to active, unmethylated rDNA loci in HeLa cells.

In addition, specific histone modifications have been implicated in maintaining active or silent rDNA loci through establishment of heterochromatic or euchromatic structures in nucleoli (25). For example, trimethylated H3 lysine 9 (H3K9me3) is essential for the maintenance of the silent chromatin state, whereas trimethylated H3 lysine 4 (H3K4me3) is a prominent mark for transcriptionally active genes (38). Thus, we next investigated whether DDX11 knockdown can affect the histone epigenetic state of rDNA loci. HeLa cells were transfected with control or DDX11-specific siRNAs, and ChIP was performed using antibodies against H3K4me3 and H3K9me3. As shown in Figure 5C, the fold enrichment of H3K4me3-associated rDNA chromatin (relative to IgG control antibody) in DDX11 siRNA-treated cells was significantly lower than that in control siRNA-treated cells.
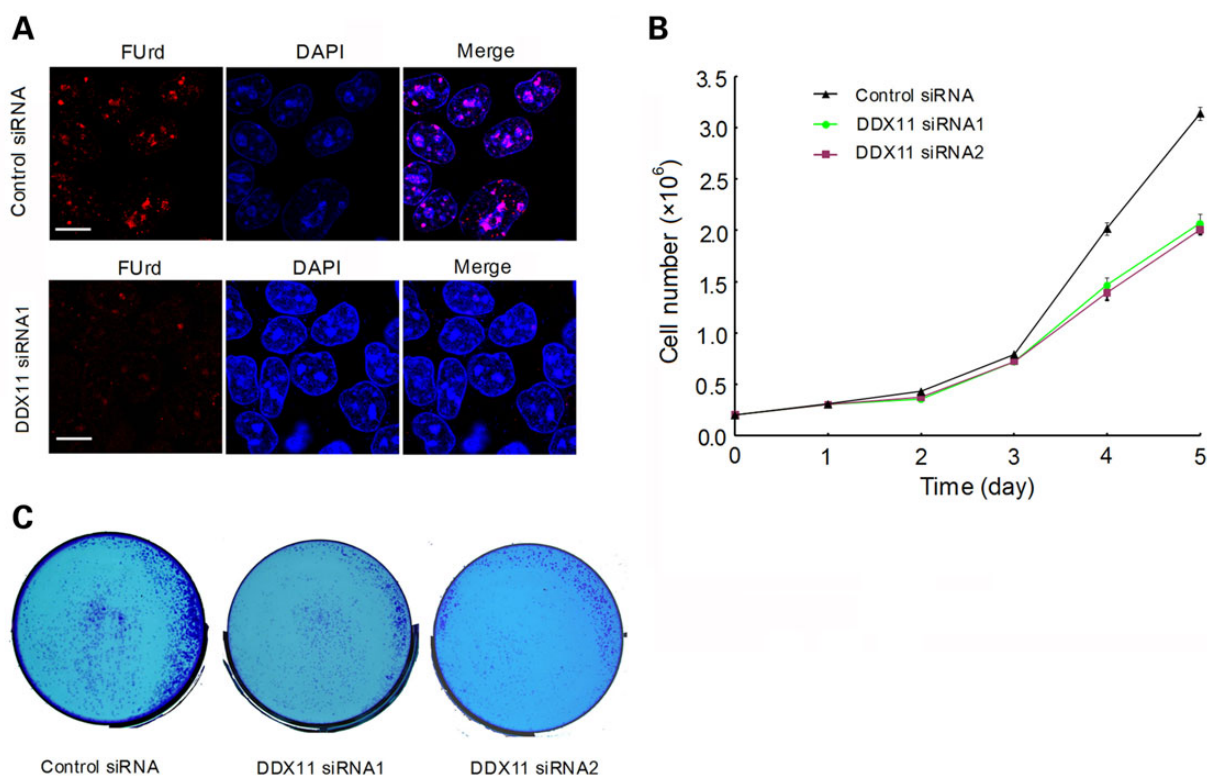
Figure 3. DDX11 knockdown suppressed cell growth and proliferation. (**A**) HeLa cells were transfected with control or DDX11-specific siRNAs for 48 h, and then pulsed with FUrd for another 15 min. Cells were fixed and stained with an anti-BrdU antibody (red). Scale bar, 10 μm. (**B**) HeLa cells were transfected with DDX11 siRNAs or control siRNA, and cell numbers were determined every 24 h. Results were expressed as mean ± SD for three replicates. (**C**) Cell colonies of HeLa cells transfected with DDX11 siRNAs or control siRNA were visualized by crystal violet staining.

In contrast, the fold enrichment of H3K9me3-associated rDNA chromatin in DDX11 siRNA-treated cells was significantly higher than that in control siRNA-treated cells (Fig. 5D). These results indicate that reduction in DDX11 levels resulted in increased heterochromatic structures at rDNA repeats.

Taken together, these data suggest that DDX11 either initiates or maintains rRNA transcription by associating with active rDNA loci as a positive regulatory factor and that loss of DDX11 results in the conversion of transcriptionally active rDNA loci to a more heterochromatic state.

DDX11 knockdown suppresses UBF activity and the recruitment of Pol I to the rDNA promoter

The presence of UBF protein is a critical determinant for rRNA transcription, and post-translational modifications of UBF, including phosphorylation at ser388 and acetylations, have been shown to be required for transcriptional activation of rDNA genes (30,31). A previous study has shown that rRNA transcription is a growth factor-stimulated process and UBF phosphorylated ser388 levels increase following serum stimulation (39). The data depicted in Figure 6A show that DDX11 knockdown markedly suppressed phosphorylation of UBF at ser388 in response to serum stimulation of HeLa cells. In order to investigate whether DDX11 can also affect the acetylation levels of UBF, immunoprecipitation experiments were performed in HeLa cells treated with control or DDX11-specific siRNAs using an antibody against acetylated lysine to detect the levels of UBF acetylation. As shown in Figure 6B, DDX11 knockdown significantly reduced the acetylation levels of UBF compared with levels of control

siRNA transfected cells. HDAC1, a member of the histone deacetylase family, has been confirmed to be able to efficiently hypoacetylate UBF both *in vitro* and *in vivo* (39,40). Previous studies have shown that trichostatin A (TSA) can specifically prevent UBF deacetylation through inhibition of HDAC1 activity (31). Consistent with previous reports, treatment of HeLa cells with TSA rescued the reduction in acetylation levels of UBF induced by DDX11 knockdown, suggesting that HDAC1 is involved in regulating UBF deacetylation in response to DDX11 knockdown (Fig. 6B). Next, we tested the effects of DDX11 knockdown on the interaction between UBF and HDAC1 using a Co-IP assay. The data in Figure 6C demonstrate that DDX11 knockdown promoted an interaction between HDAC1 and UBF in HeLa cells.

Several studies have shown that the acetylation and phosphorylation of UBF are important for its binding to rDNA promoter, as well as for the recruitment of RNA polymerase I complex and the transcriptional activity of rDNA (41–44). Consistent with the observed changes in UBF phosphorylation and acetylation levels, results of the ChIP assays examining the rDNA promoters using UBF and RPA194 antibodies showed that depletion of DDX11 also significantly suppressed the binding of UBF (Fig. 6D) and RPA194 (Fig. 6E) to rDNA loci.

Mutations of DDX11 affect the binding to rDNA and enzyme activity

DDX11 contains a DEAD/DEAH box, a Fe–S domain and seven conserved helicase domains (Fig. 7A). All helicases possess DNA-binding activity that is driven by ATP, because the energy from ATP hydrolysis is necessary to promote their helicase activities.
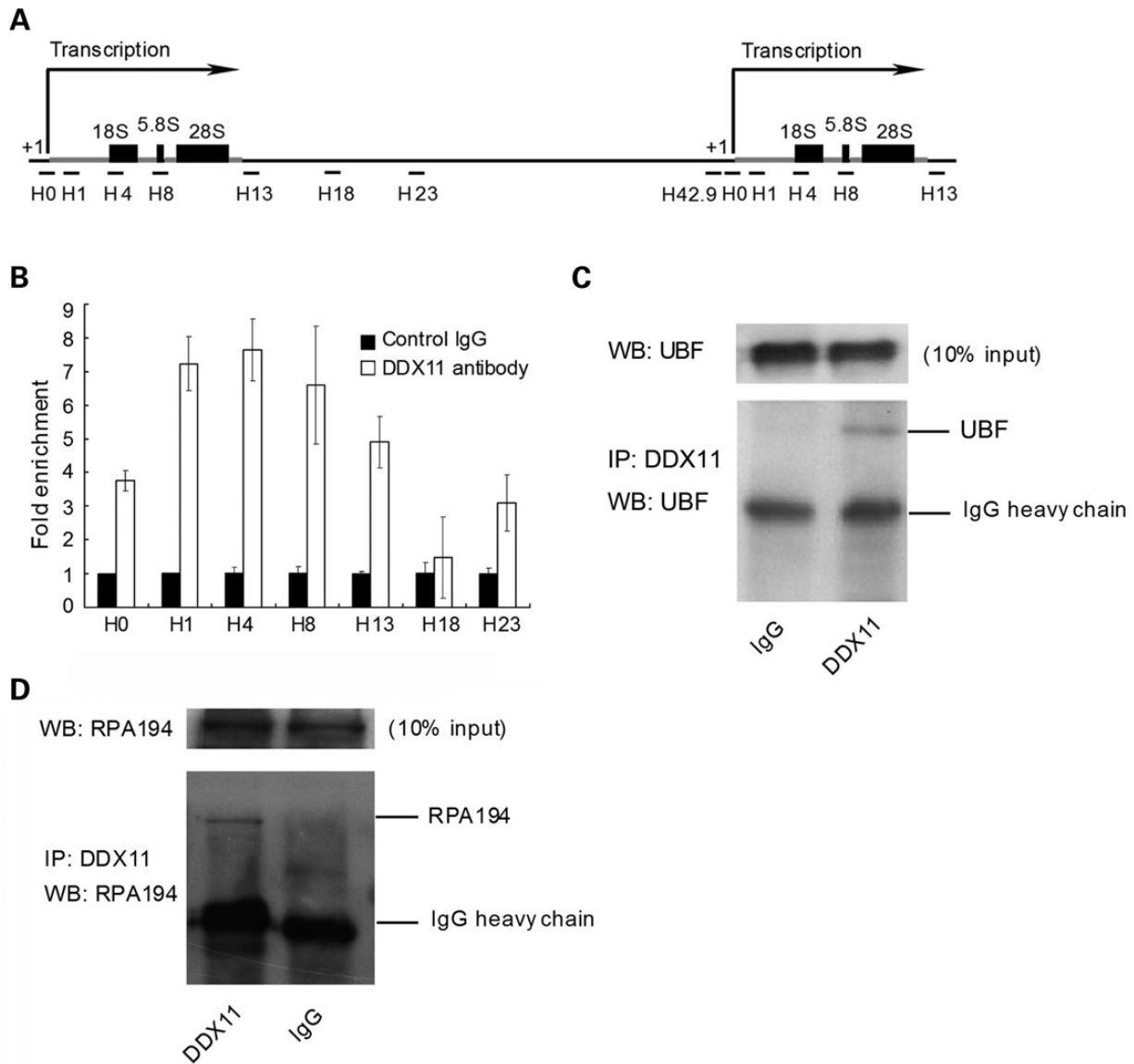
Figure 4. DDX11 occupied rDNA loci and associated with Pol I transcriptional complexes. (**A**) Schematic illustration of a single human rDNA repeat and the positions of primers used for ChIP. The numbers for positions are the distances (kb) from the transcriptional start site across the rDNA loci. (**B**) ChIP assay was performed with control IgG or DDX11 antibodies and the precipitated DNA was analyzed using qPCR with the described primers in (A). The enrichment of IgG treatment was set to 1, and the data from samples treated with DDX11 antibody were expressed as relative fold-enrichments of IgG treatment. Error bars represent the SD of three independent experiments. (**C**) and (**D**) Endogenous DDX11 protein was immunoprecipitated using anti-DDX11 antibody and mouse IgG was used to reduce non-specific binding. The co-precipitated UBF and RPA194 were examined by western blotting using anti-UBF and anti-RPA194 antibodies, respectively.

Because DDX11 mutations have been associated with WABS, we compared the binding abilities to an rDNA promoter and the ATPase activities of wild-type DDX11, two WABS patient-derived mutants (R263Q and K897del) and a Fe–S deletion construct *in vitro* (Fig. 7A). As shown in Figure 7B, R263Q and K897del mutants showed significantly decreased binding abilities on an rDNA promoter fragment compared with the wild-type DDX11. A construct containing a deletion of the Fe–S domain also showed significantly diminished binding abilities, indicating that the Fe–S domain is vital for DDX11 interactions with rDNA loci (Fig. 7B). In addition, DNA-dependent ATPase activity assays showed that the DDX11 mutant proteins demonstrated significantly lower enzyme activities compared with wild-type proteins (Fig. 7C).

The effects of DDX11 mutants on rDNA promoter activities were further investigated *in vivo* using a luciferase assay as described in the *Materials and Methods* section. As shown in Figure 7D, cells that overexpressed mutant DDX11 proteins demonstrated significantly reduced luciferase activities compared with cells that overexpressed wild-type DDX11. These results indicated that DDX11 mutations identified in WABS patients affect the ability of DDX11 to promote rDNA transcription.

zDDX11 knockdown leads to the craniofacial and vertebrate development defects of zebrafish

DDX11 mutations were recently associated with WABS. However, because the DDX11-null mutation is embryonically lethal in a knockout mouse model, no DDX11 loss-of-function phenotype analyses have been reported. In order to examine the *in vivo* phenotype of DDX11 mutations, we used a zebrafish model to
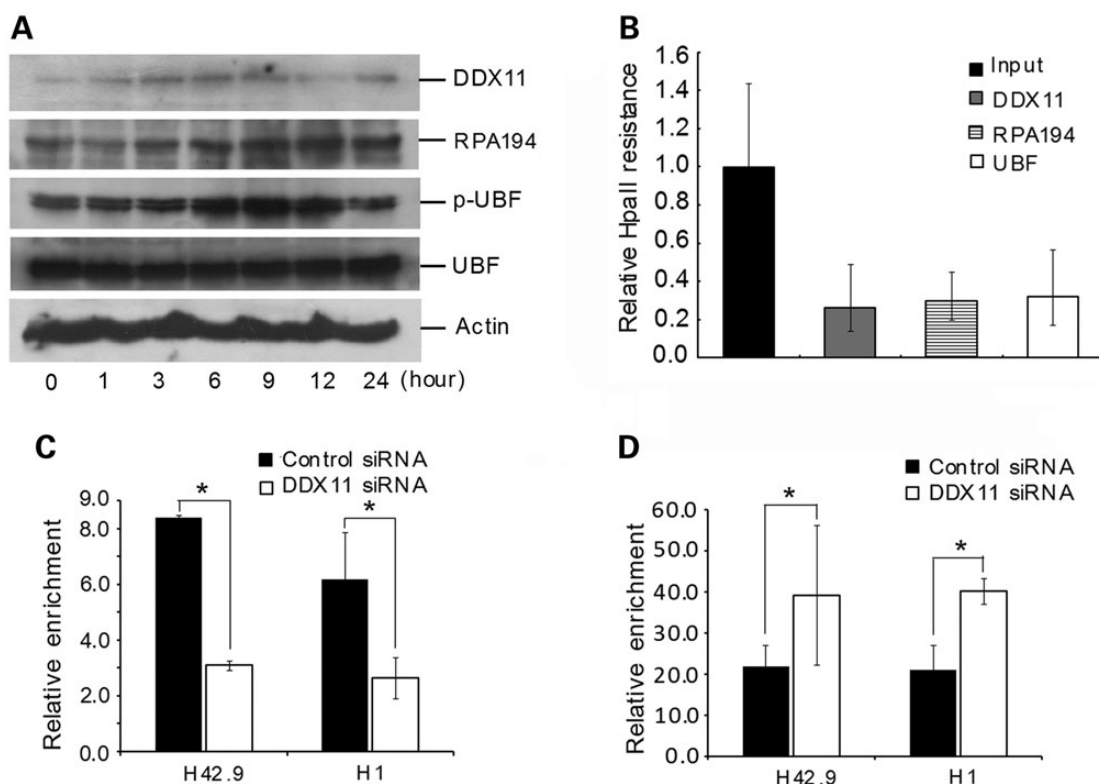
Figure 5. DDX11 bound to active rDNA loci as a positive regulation factor. (**A**) HeLa cells were serum starved for 48 h and then stimulated with 15% serum for the indicated times. Cell lysates were subjected to western blotting using antibodies against the indicated antibodies. (**B**) DNA isolated using ChIP was digested with Hpa II, and then subjected to qPCR analysis using primers flanking an HpaII site within the rDNA promoter region. The Hpa II resistance was calculated after normalization to mock-digested DNA. Data from input were set to 1, and data from other samples were expressed as relative Hpa II resistance. (**C**) and (**D**) Control or DDX11-specific siRNAs were transfected into HeLa cells and ChIP assays were performed with H3K4me3 or H3K9me3 antibodies. The precipitated DNA was subjected to qPCR analysis using H1 and H42.9 primers targeting the promoter region of rDNA, and the data were expressed as relative fold-enrichments of IgG treatment. Data from three independent experiments are presented as mean ± SD (*$P < 0.05$).

investigate the phenotype resulting from loss of DDX11 during zebrafish development. Co-injections of control morpholino or zDDX11 morpholinos together with a GFP-fused plasmid containing the morpholino-targeted sequences confirmed the knockdown effectiveness and specificity of the zDDX11 morpholinos (data not shown). A control morpholino, 5′UTR morpholino or ATG morpholino of zDDX11 mRNA were injected into zebrafish embryos at the single-cell stage in doses of 6, 9 and 12 ng/embryo, respectively. One hundred of embryos were injected for each treatment group, and the morphology was observed at 3 d.p.i. As shown in Figure 8A, 5′UTR morpholino and ATG morpholino significantly increased the embryonic lethality in a dose-dependent manner. Moreover, injections of zDDX11-specific morpholinos resulted in significant developmental abnormalities in zebrafish, when compared with that in the control morpholino-treated group, with the most pronounced defects in craniofacial and vertebrate development at 3 d.p.i (Fig. 8A). As shown in Figure 8B, zebrafish embryos from the zDDX11 morpholino-treated group at 3 d.p.i. exhibited shortened and twisted torsos, smaller eyes and low mouth positions (arrows). With increasing time following injections, zDDX11 morpholino-treated zebrafish showed more obvious craniofacial defects, including longer faces, low and protuberant mouths and narrow eye distances at both 5 and 7 d.p.i. (Fig. 8C–E), which have similarities to the congenital abnormalities described in WABS patients (8).

We have showed that DDX11 knockdown can change the epigenetic state of rDNA loci, affect the recruitment of Pol I to

rDNA promoter and suppress rRNA transcription in HeLa cells. To further confirm this finding in the zebrafish model, ChIP assays were performed to investigate the epigenetic changes of rDNA loci using H3K4me3 and H3K9me3 antibodies at 48 h post-injection of control or zDDX11 morpholino. Similar to the results observed in HeLa cells, the fold enrichment of H3K4me3-associated rDNA chromatin (relative to IgG control antibody) in zDDX11 morpholino-treated zebrafish embryos was significantly lower than that in the control morpholino-treated zebrafish embryos (Fig. 8F). In contrast, the fold enrichment of H3K9me3-associated rDNA chromatin in zDDX11 morpholino-treated zebrafish embryos was significantly higher than that in the control morpholino-treated zebrafish embryos (Fig. 8F). These results indicate that zDDX11 knockdown also resulted in increased heterochromatic structures at rDNA repeats. Expectedly, ChIP assays examining the zebrafish rDNA promoter using zebrafish polr1a (DNA-directed RNA polymerase I largest subunit) antibody showed that depletion of zDDX11 also significantly suppressed the recruitment of polr1a to rDNA loci (Fig. 8G). Furthermore, the pre-rRNA levels in embryos microinjected with the zDDX11-specific morpholinos were measured using qPCR and compared with those found in control embryos. zDDX11 knockdown significantly reduced pre-rRNA levels in zebrafish embryos (Fig. 8H).

Together with our *in vitro* data, these results suggest that the developmental defects induced by zDDX11 knockdown in zebrafish are at least partially associated with nucleolar dysfunction.
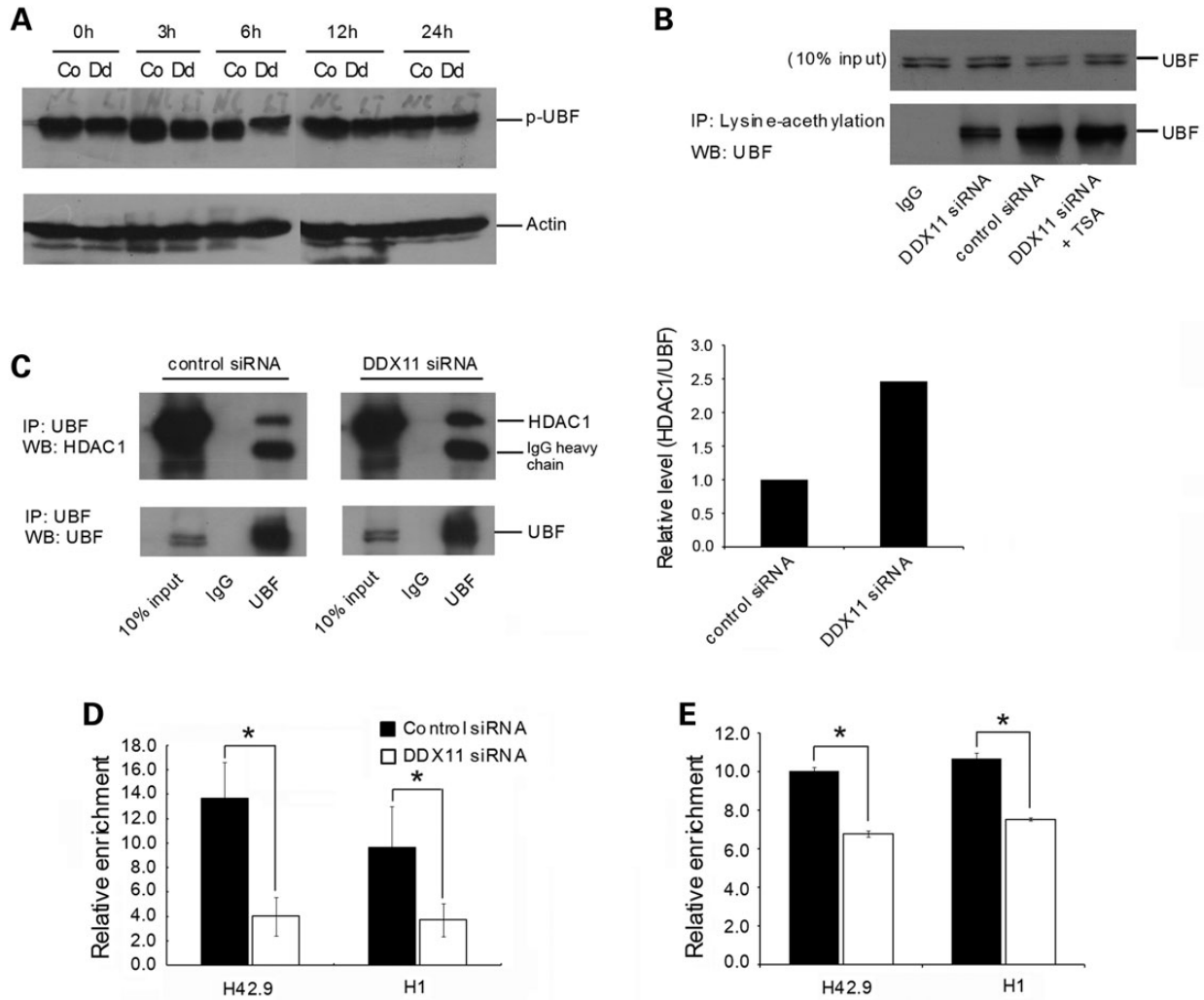
Figure 6. DDX11 regulates UBF activity and its recruitment to the rDNA loci. (**A**) HeLa cells transfected with control (Co) or DDX11-specific siRNA (Dd) were serum starved for 48 h and then stimulated with 15% serum for the indicated times. Cell lysates were subjected to western blotting using antibodies against the indicated antibodies. (**B**) Cells were treated with control or DDX11-specific siRNA in the presence or absence of TSA, co-IP was performed using acetylated-lysine antibodies, and UBF was detected by western blotting. (**C**) Immunoprecipitation analysis demonstrated that DDX11 knockdown increased the interactions between HDAC and UBF, when compared with that of the control siRNA treatment. *Columns:* the immuneprecipitated HDAC1 was quantified by densitometric analysis of blots, and normalized to UBF. The relative levels of HDAC1/UBF in control and DDX11 siRNA groups were compared (the relative level of HDAC1/UBF in control group was set to 1). (**D**) Cells were treated with control or DDX11-specific siRNA, and equal amounts of the cell lysates were subjected to ChIP using anti-UBF or IgG antibodies. The precipitated DNA was analyzed using qPCR with the primers of H42.9 and H1. Data from three independent experiments were expressed as relative fold-enrichments of IgG treatment (*$P < 0.05$). (**E**) Similar to (**D**), the precipitated DNA using anti-RPA194 or IgG antibodies was analyzed using qPCR with primers of H42.9 and H1 (*$P < 0.05$).

Discussion

WABS was originally identified as a new form of cohesinopathy in a patient that presented clinically with several congenital abnormalities, including pre- and postnatal growth retardation, microcephaly, facial dysmorphy (small and elongated face, relatively large mouth and narrow bifrontal diameter), high arched palate, clinodactyly and mild mental retardation. This patient and his parents carry a splice site mutation (c.2271+2T>C) and a C-terminal deletion mutation (K897del) in the DDX11 gene (8). Subsequently, a novel homozygous mutation (R263Q) in the DDX11 gene was identified in three affected siblings from a Lebanese family that presented with many of the same congenital abnormalities as the first reported WABS patient, but with more severe intellectual disabilities (9).

Previous studies indicated that DDX11 is involved in the maintenance of genomic stability and cohesion of the chromosome arms and centromeres in nucleocytoplasm or in mitotic phase (Fig. 9) (11–15,17,18). Here, we provide novel evidence that DDX11 is also constitutively localized to the nucleoli in interphase cells and functions as a positive regulator of rRNA biogenesis. Nucleoli are the sites of pre-rRNA transcription, rRNA processing and ribosome subunit assembly (20,21). Recently, a growing body of evidence has indicated that nucleoli also participate in many other biological processes, including the cell cycle, cell growth and death, stress responses, aging, development and even human diseases (32–34,45). In particular, mutations in several nucleoli-localized proteins have been linked to the human family genetic syndromes, such as Roberts syndrome (46), Werner syndrome (47), Börjeson–Forssman–Lehmann syndrome (48), Shwachman–Diamond syndrome (49), Bowen–Conradi syndrome (50), CHARGE syndrome (27), Woodhouse–Sakati syndrome (51) and Siderius–Hamel CL/P syndrome (52). Most of these nucleoli-localized
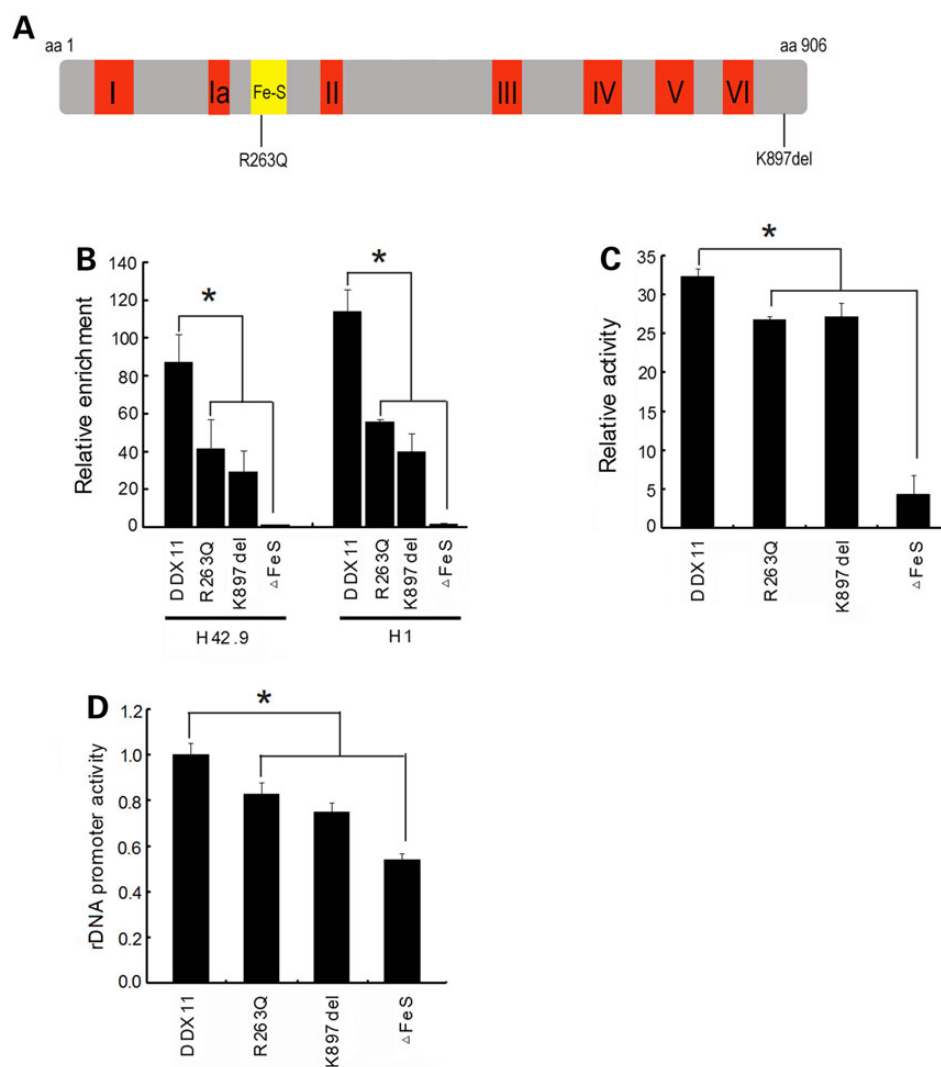
Figure 7. DDX11 mutations affect its binding to rDNA promoters and ATPase activity. (**A**) A schematic representation of DDX11 protein indicating a Fe–S domain, seven conserved helicase motifs and two identified mutations in WABS patients. (**B**) An *in vitro* binding assay was performed as described in *Materials and Methods*. The data were expressed as relative fold-enrichments of control treatment (*P < 0.05). (**C**) DNA-dependent ATPase activity of wild-type of DDX11 and its mutants were measured using an ATPase detection kit. Data from three independent experiments were expressed as relative enzyme activity (*P < 0.05). (**D**) The effect of DDX11 mutants on rDNA promoter activity was investigated using dual-luciferase reporter assays. The activity of wild-type DDX11 was set to 1, and the data of mutant proteins were expressed as relative rDNA promoter activity. Bars represent the SD of three independent experiments (*P < 0.05).

proteins have been shown to regulate ribosome biogenesis, and mutations in these proteins can result in nucleolar dysfunction during rRNA transcription. For example, mutations in plant homeodomain finger protein 8 (PHF8) have been shown to cause Siderius–Hamel CL/P syndrome, a newly diagnosed X-linked mental retardation syndrome characterized by facial dysmorphism, cleft lip and/or palate, and microcephaly (52,53). PHF8 can regulate rRNA transcription through interactions with WDR5-containing H3K4 methyltransferase complexes and with the RNA Pol I complex. Mutations in PHF8 identified clinically abolish its nuclear localization, demethylase activity and rRNA transcriptional activation, linking nucleolar dysfunction to genetic disease (29,54). In this study, we show that DDX11 is a novel nucleolar protein that preferentially binds to active rDNA gene loci. DDX11 knockdown resulted in a change in the epigenetic state of rDNA loci from euchromatic structures to more heterochromatic structures. As DDX11 possesses classical helicase domains, we proposed that DHX11 might alter the rDNA chromatin structure through its DNA binding and helicase activities. In addition, DDX11 is also a crucial interaction partner for UBF and RNA Pol I transcriptional machinery. UBF is an rDNA chromatin-modulating protein and can bind across rDNA promoters to activate rRNA transcription (22). As we hypothesized, DDX11 knockdown affected the phosphorylation and acetylation of UBF, as well as its recruitment to rDNA promoters, leading to suppressed rRNA transcription. Thus, our findings provide novel insights into the functions of DDX11 in normal cells, and link the functions of DDX11 in nucleoli to WABS.

DDX11 belongs to the DEAD/DEAH-box proteins in the helicase family that consists of about 50 members. DEAD/DEAH-box helicase superfamily was generally believed to function in RNA metabolism, including transcriptional regulation, pre-mRNA splicing, nucleocytoplasmic transport, translation and mRNA decay by through potential RNA helicase activity (55). However, some members of this superfamily, such as DHX9 and DHX33, have been also shown to function as DNA helicases and to regulate rRNA transcription (37,56). For example, Zhang
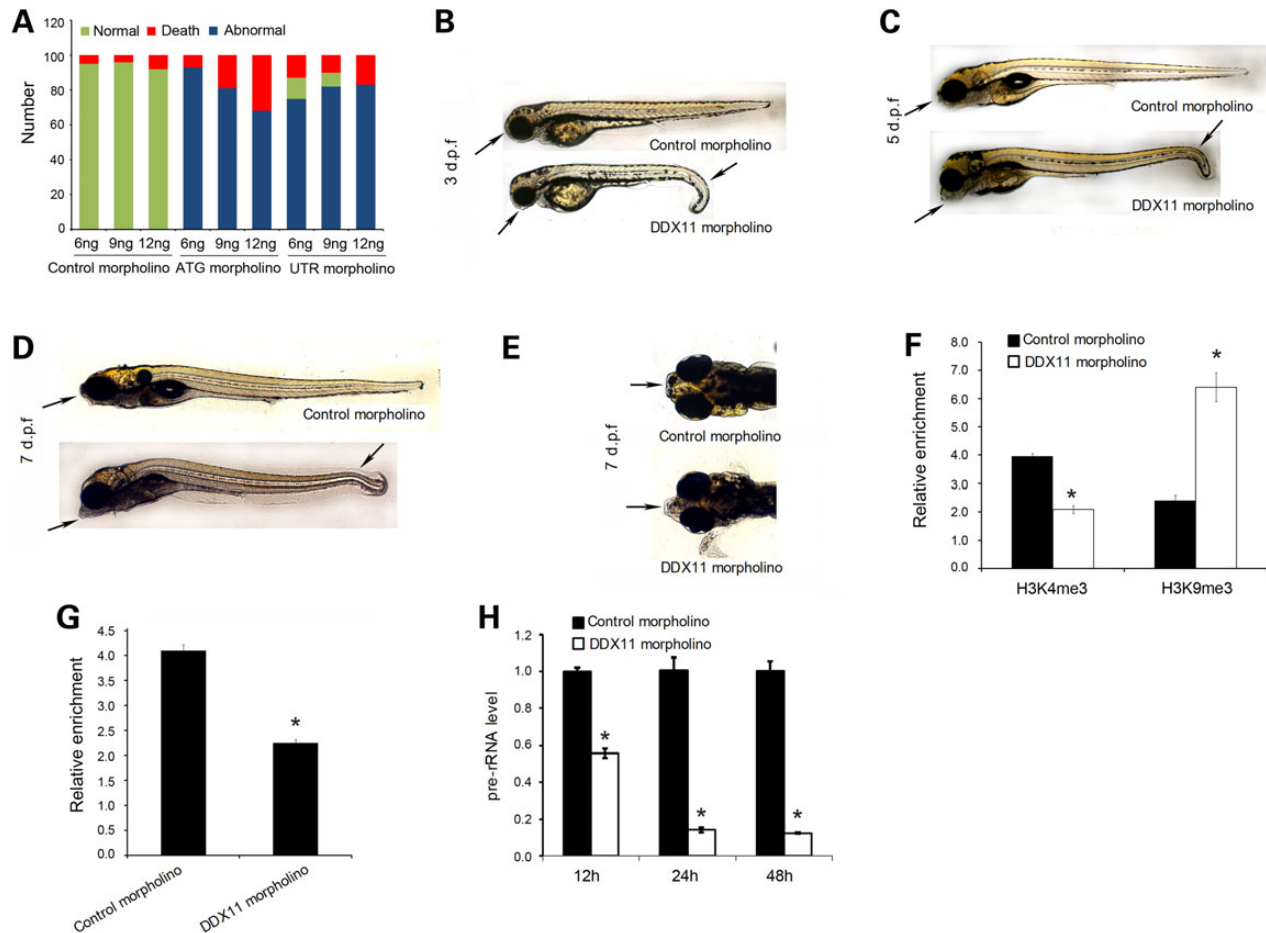
Figure 8. DDX11 knockdown affects the development of zebrafish. One hundred of embryos were injected using control or zDDX11 morpholinos at doses of 6, 9 and 12 ng/embryo. (**A**) The number of dead embryos and the zebrafish with normal morphology and abnormal morphology were counted at 3 d.p.i, and the representative phenotypes of the zebrafish at 3 (**B**), 5 (**C**) and 7 d.p.i. (**D** and **E**) were shown. Arrows indicate the sites with developmental defects compared with zebrafish in the control group. (**F**) ChIP assays were performed using H3K4me3 or H3K9me3 antibodies at 48 h post-injection of control or zDDX11 morpholino. The precipitated DNA was subjected to qPCR analysis using primers targeting the promoter region of zebrafish rDNA, and the data were expressed as relative fold-enrichments of IgG treatment. Data from three independent experiments are presented as mean ± SD (*$P < 0.05$). (**G**) ChIP assay was performed with anti-zebrafish polr1a antibody at 48 h post-injection of control or zDDX11 ATG morpholino. The precipitated DNA was subjected to qPCR analysis using the primers targeting the promoter region of zebrafish rDNA, and the data were expressed as relative fold-enrichments of IgG treatment. Data from three independent experiments is presented as mean ± SD (*$P < 0.05$). (**H**) The pre-rRNA levels in embryos with control or zDDX11 morpholino injection at 12, 24 and 48 h post-injection were detected by qPCR. The relative pre-rRNA level in the control group was set to 1 (*$P < 0.05$).

et al. investigated the potential roles of 28 putative RNA helicases within DEAD/DEAH family in the regulation of rDNA transcription using a shRNA deletion screen. This screen identified DHX33 as an important regulator of rDNA transcription, because DHX33 knockdown resulted in a 10-fold decrease in 47S pre-rRNA levels (37). Similarly, we show that DDX11 knockdown also results in approximately 5-fold reduction in 47S pre-rRNA levels (Fig. 2). Moreover, DDX11 specifically binds to rDNA promoters (Fig. 4) and demonstrates DNA-dependent ATPase activity (Fig. 7). Two bi-allelic mutations (K897del and R263Q) of DDX11 gene associated with WABS have been independently identified in a male individual from Warsaw, Poland and three affected siblings from Lebanon (7–9). Some *in vitro* biochemical studies showed that these two clinically relevant mutations impaired DDX11 helicase activity by perturbing the DNA binding and DNA-dependent ATPase activity (8,9). Similar to these findings, R263Q and K897del were also demonstrated to have significantly reduced binding abilities on rDNA promoters and lower DNA-dependent ATPase activities, resulting in reduced rRNA transcriptional

rates compared with those of wild-type DDX11 (Fig. 7). Therefore, we speculated that inefficient unwinding of rDNA duplexes caused by DDX11 mutations reduced UBF recruitment, rDNA occupancy of the RNA Pol I machinery and rRNA transcription. These observations further deepened our understanding of the novel biological functions of proteins in the DEAD/DEAH box helicase family. Further, our results also suggest that nucleolar dysfunction caused by DDX11 mutations is involved in WABS pathogenesis.

Homologs of the human DDX11-encoded gene appear to be highly conserved in evolution from yeast to humans. To fully understand the potential functions of DDX11 during development and in WABS pathogenesis, the DDX11 gene was knocked out in a mouse model. However, the DDX11-null mice died at embryonic day 10.5, which was attributed to developmental abnormalities in the placenta (14). Subsequently, Cota *et al.* generated a null allele mutation in the motif V of DDX11 protein using N-ethyl-N-nitrosourea (ENU) in mice (19). Unfortunately, the mutant embryos also appeared to stop developing at E8.5 and
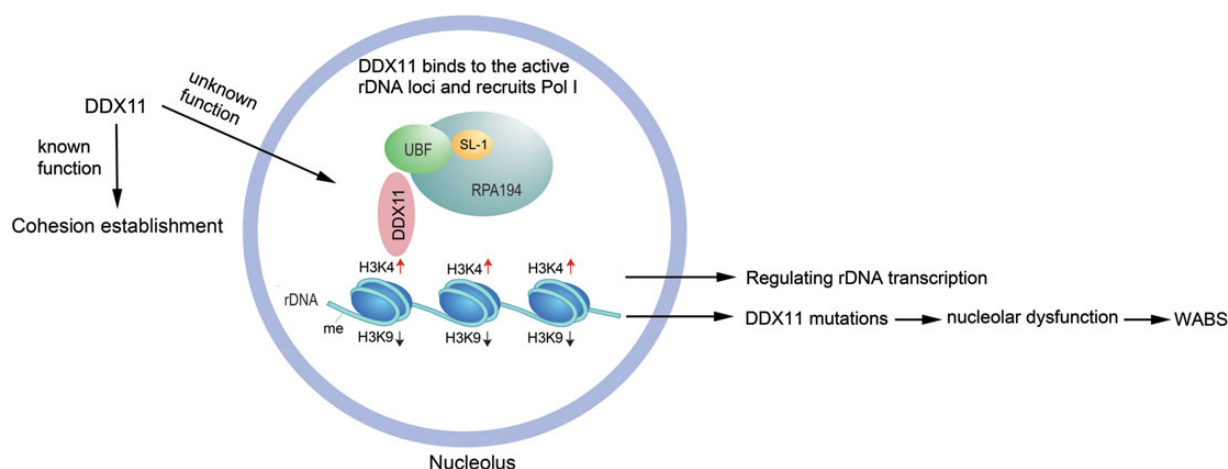
Figure 9. Proposed model for the novel role of DDX11 in nucleoli. DDX11 has been known to function in the cohesion of chromosome arms and centromeres in mitosis. Here, DDX11 was identified as a novel nucleolar-localized protein in interphase, which can promote rRNA transcription by binding to active rDNA gene loci and recruiting UBF and RNA Pol I transcriptional machinery. Mutations in DDX11 reduce its binding ability to rDNA promoter and DNA-dependent ATPase activity, affect the UBF activity, and decrease the recruitment of Pol I complex and rRNA transcriptional rate. Consequently, nucleolar dysfunction results in specific developmental defects in zebrafish embryos and WABS.

showed similar placental defects to that described in DDX11-knockout embryos (19). Although these results indicated DDX11 is vital for mouse embryonic development, the phenotypes of both mouse models cannot be observed due to early embryonic death. In this paper, we used zebrafish as a model to investigate the effects of zDDX11 loss on zebrafish development and phenotypes. zDDX11 knockdown by morpholinos resulted in craniofacial and vertebrate defects with shortened and twisted torsos, longer faces, smaller eyes, low and protuberant mouths and narrowed eye distances (Fig. 8A–E), which have similarities to the spectrum of pathology observed in WABS patients (8,9). Moreover, zDDX11 knockdown also resulted in the changes in histone epigenetic modifications at rDNA loci (Fig. 8F), the reduction of Pol I recruitment to the rDNA promoter (Fig. 8G) and a significant decrease in nascent pre-RNA levels (Fig. 8H) in zebrafish embryos, suggesting that the development and phenotype defects observed in these zebrafish is associated with nucleolar dysfunction caused by zDDX11 knockdown. Thus, we generated a DDX11-deficient animal model with similarities to WABS-related phenotypes for the first time in any vertebrate.

Several studies have demonstrated that depletion of DDX11 caused mitotic failure with abnormal sister chromatid cohesion and chromosome segregation defects, consistent with observations described in the clinical WABS (8,13,14). The clinical symptoms of WABS are partially overlapped with Cornelia de Lange syndrome and Roberts syndrome (RBS), the other two cohesinopathies, characterized by facial and skeletal abnormalities, growth retardation, intellectual disability and so on (57). Therefore, our results could not exclude the possibility that the developmental abnormality of zebrafish is also partially attributed to the DDX11 deficiency-induced cohesion and chromosome segregation defects. However, the nucleolar defects are also observed in RBS. Mutation of the cohesin acetyltransferase in RBS is associated with impaired rRNA transcription and ribosome biogenesis in yeast and human cells. Mutations in other subunits of the cohesin ring are also associated with defects in nucleolar function, demonstrating that maintenance of cohesion is critical for nucleolar function (46,58,59). In addition, several acknowledged nucleolar proteins were found to play important roles in sister chromatid cohesion, centrosome and chromosome segregation at G2/M phase (60–67), and several centromeric

components or proteins also accumulated in human interphase nucleolus in an RNA polymerase I-dependent manner (68,69). All of these findings indicate that nucleolus is associated with sister chromatid cohesion and chromosome segregation, and WABS might be caused by the comprehensive effect of the DDX11 deficiency-induced nucleolar dysfunction, abnormal cohesion and chromosome segregation defect.

Taken together, our data identified a novel nucleolar-localized protein, DDX11, as an important positive regulator of rRNA transcription (Fig. 9). DDX11 preferentially binds to hypomethylated active ribosomal rDNA gene loci, where it interacts with UBF and RNA Pol I transcriptional machinery. DDX11 knockdown changed the epigenetic state of rDNA chromatin from euchromatic structures to more heterochromatic structures, suppressed UBF activation and Pol I recruitment to rDNA promoters, and reduced rRNA transcriptional levels. Importantly, clinically identified mutants of DDX11 affected rRNA transcriptional rates owing to their significantly weaker binding abilities to rDNA promoters and lower DNA-dependent ATPase activities compared with those of wild-type DDX11, linking nucleolar dysfunction to the pathology of WABS. Moreover, zDDX11 knockdown resulted in reduced rRNA expression and WABS-like symptoms in a zebrafish model for the first time, further supporting previous reports that DDX11 mutations might be the underlying cause of WABS. Thus, our findings provide novel insights into the cellular role of DDX11 in normal cells and WABS pathogenesis beyond its previously identified functions in sister chromatid cohesion and maintenance of genomic integrity (Fig. 9).

Materials and Methods

Cell lines, plasmids, siRNAs, morpholinos and antibodies

HEK293 and HeLa cells were purchased from American Type Culture Collection (ATCC) and cultured in DMEM supplemented with 10% fetal calf serum (Hyclone, Logan, UT, USA), 100 units/ml penicillin and 100 μg/ml streptomycin. Human DDX11 and two clinical mutants (R263Q, K897del), and a Fe–S domain deletion mutant (ΔFe–S) were cloned into the pFLAG-CMV2 vector (Sigma–Aldrich, St. Louis, MO, USA). The pHrD-IRES-Luc plasmid containing the promoter sequence for the rDNA gene was a kind

gift from professors Ke Y and Jacob ST (70,71). Chemically synthesized siRNAs specifically targeting human DDX11 were purchased from GenePharma (Shanghai, China). The sequences of siRNA1 and siRNA2 were 5′-GAAGAAGAGGCACGACUCCTT-3′ and 5′-GCAGGCACGAGAAGAAGAATT-3′, respectively. Two morpholinos targeting the 5′ UTR region from −69 to 45 and the ATG region from −2 to +23 of zebrafish DDX11 mRNA were synthesized by Gene Tools (Philomath, OR, USA). To evaluate the effectiveness of the morpholinos, a GFP-fused DNA fragment containing morpholinos target sequences was constructed into PCS2+ vector (Addgene, Cambridge, MA, USA). The primary antibodies for p-UBF (ser 388), RPA194, nucleolin, DDX11, FLAG, BrdU and β-actin were purchased from Santa Cruz Biotechnology (Santa Cruz, CA, USA). The primary antibody for UBF was obtained from Cell Signaling (Beverly, MA, USA). H3K4me3 and H3K9me3 antibodies were obtained Milipore (Bedford, MA, USA). HRP- and fluorescein-labeled secondary antibodies and the ECL detection system were purchased from KPL (Gaithersburg, MD, USA). Anti-zebrafish polr1a antibody was from Ab-mart (Berkeley Heights, NJ, USA). Anti-FLAG M2 affinity gels (Sigma–Aldrich) were used to precipitate FLAG-fused proteins. ChIP assays were performed using Dynabeads Protein G magnetic beads (Life Technologies, Carlsbad, CA, USA).

Nucleolus fractionation

Nucleoli isolation from HeLa cells was performed as described previously (72). An equal amount of protein isolated from nuclear and nucleolar fractions was subjected to western blotting.

Quantitative PCR for pre-rRNA expression

Total RNA from HeLa and HEK293 cells and zebrafish embryos was extracted using TRIzol regent (Invitrogen Corp., Carlsbad, CA, USA) according to the manufacturer's specifications. The cDNA was synthesized by reverse transcription using random primers, and the product was used to analyze pre-rRNA expression using SYBR Green real-time quantitative PCR (qPCR). Primers for human and zebrafish pre-rRNA detection used for qPCR were synthesized as described in previous reports (54,73,74).

Luciferase reporter assay

To evaluate the effects of DDX11 knockdown on rDNA promoter activity, HeLa or HEK293 cells grown on 12-well plates were transfected with DDX11-specific or control siRNAs for 24 h, followed by the addition of 1 μg pHrD-IRES-Luc and 50 ng pRL-TK into the media. Cells were incubated for 24 h and then harvested in the passive lysis buffer. The relative rDNA promoter activity was measured in cell lysates using a dual-luciferase assay kit (Promega, Madison, WI, USA). To evaluate the effects of wild-type DDX11 and its mutants on rDNA transcription, HeLa cells were transfected with DDX11-specific siRNA for 24 h, followed by the addition of 1 μg pFLAG-CMV2 plasmid containing DDX11 or its mutant gene together with 500 ng pHrD-IRES-Luc and 50 ng pRL-TK with the cells for another 24 h. Cells were harvested, and the relative rDNA promoter activities were measured as described above.

Immunofluorescence and 5-fluorouridine (FUrd) incorporation assay

HeLa and HEK293 cells grown on glass coverslips were fixed using pre-chilled methanol for 10 min and then permeabilized for 15 min with 0.1% Triton X-100 in PBS at room temperature. Cells were washed three times with PBS and blocked with 1%

BSA in PBS for 1 h at 4°C. After incubation with primary antibodies against DDX11 and nucleolin at 4°C overnight, the coverslips were incubated with fluorescein or rhodamine-conjugated secondary antibodies for 1 h at room temperature. Nuclei were counterstained with DAPI. Finally, cells were examined and imaged using a confocal microscope.

To monitor nascent rRNA, an FUrd incorporation assay was performed. Briefly, DDX11 siRNA1 or control siRNA was used to transfect HeLa or HEK293 cells grown on coverslips in a six-well culture plate. FUrd (Sigma–Aldrich) was added 24 h after transfection at a final concentration of 10 mM. After 15 min incubation, cells were subjected to immunodetection with an anti-bromodeoxyuridine (BrdU) antibody.

Co-immunoprecipitation assay (Co-IP)

HEK293 cells were resuspended in IP buffer (20 mM Tris–HCl pH 8.0, 150 mM NaCl, 1 mM EDTA, 1 mM EGTA, 1% Triton X-100, protease inhibitor cocktail) and subjected to sonication for 10 s. The cell lysates were clarified using centrifugation at 16 000 rpm for 15 min. Protein extracts were then mixed with the indicated primary antibodies and protein A/G agarose (Sigma, St. Louis, MO, USA) for 4 h at 4°C. The complexes were collected and washed three times with IP buffer. The resolved proteins were analyzed using western blotting (75,76).

Chromatin immunoprecipitation

ChIPs were performed in accordance with a published protocol (77) with minor modifications. Briefly, cells were fixed with 1% formaldehyde for 15 min at room temperature, and cross-linking reactions were then quenched by adding 125 mM glycine for 5 min. After washing the cells with PBS, the cells were collected and resuspended in ChIP lysis buffer (50 mM Tris–HCl pH 7.5, 150 mM NaCl, 5 mM EDTA, 0.5% NP-40, 1.0% Triton-X-100 and protease inhibitor cocktail), then subjected to sonication to produce 200–1000 bp DNA fragments. Sheared chromatin was immunoprecipitated with the indicated antibodies or control IgG in combination with Dynabeads Protein G magnetic beads. After several washes, beads were resuspended with Chelex 100 suspension and boiled for 10 min. After the tubes cooled on ice, proteinase K was added. The tubes were then incubated in a shaker (1 h, 55°C at 1400 rpm) followed by boiling for 10 min. After centrifugation, the suspension was collected to perform qPCR analysis, and fold enrichment relative to the IgG control antibody was calculated. Primers (H0, H1, H4, H8, H13, H18, H23, H42.9) for rDNA loci used in the ChIP assays were synthesized as specified by a previous report (78). The primers targeting the promoter region of zebrafish rDNA in the ChIP assays are as follows: 5′-CCGGT CTACCTCGAAAGTC-3′ and 5′-CGAGCAGAGTGGTAGAGGAAG-3′.

Assay for colony formation

HeLa cells were transfected in suspension with DDX11-specific siRNAs or control siRNA and then plated on six-well plates. Cells were cultured for 14 days. Colonies were photographed after staining with 5% crystal violet for 10 min.

Cell proliferation assay

Cells were transfected with DDX11-specific siRNAs or control siRNA and then seeded at low density (100 000 cells/10 cm plate). Cell numbers were quantified every day, and the data from three independent studies were presented as mean ± standard deviation (SD).

ChIP-chop assay

ChIP was performed on HeLa cells using antibodies for FLAG-DDX11, RPA194 and UBF, and aliquots of chromatin from ChIP and input samples were digested or not digested (mock-digested) with HpaII, a methylation-sensitive enzyme that cannot cut methylated CCGG sequences. qPCR was utilized to detect the rDNA promoter region (–157/+43) in the input and ChIP samples that contained HpaII sites using the primer pairs described previously (27). The relative resistance to HpaII digestion was calculated following normalization to mock-digested DNA.

In vitro binding analysis of rDNA promoter

HEK293 cells were transfected with FLAG-fused DDX11 and its mutant plasmids. The cells were collected and resuspended in IP buffer, then subjected to sonication 48 h after transfection. FLAG-fused proteins were purified using anti-FLAG M2 Affinity gels. Anti-FLAG M2 Affinity gels with FLAG-fused proteins bound were then incubated with the promoter fragment of rDNA (–410 to +81) in binding buffer (20 mM HEPES pH 7.5, 25 mM KCl, 2 mM $MgCl_2$, 1 mM DTT, 1 mM ATP) at 37°C for 2 h, with an equal amount of M2 gel without bound FLAG-fused proteins used as a control. Anti-FLAG M2 Affinity gels were collected and DNA was recovered using phenol/chloroform extraction and ethanol precipitation. qPCR was performed using the H0 primer pair, and fold enrichment relative to the control was calculated.

ATPase assay

The DNA-dependent ATPase activities of DDX11 and its mutants were measured using an ATPase assay kit (Bioassay, Hayward, CA, USA). Briefly, FLAG-fused DDX11 and its mutants were produced in HEK293 cells and purified using anti-FLAG M2 Affinity gels in accordance with a previous report (10). Equal amounts of FLAG-fused proteins and promoter fragments of rDNA (–410 to +81) were used to quantify the DNA-dependent ATPase activities in assay buffer provided by the kit according to the manufacturer's instructions.

Zebrafish DDX11 (zDDX11) knockdown and phenotype analysis

To eliminate zebrafish DDX11 function, two morpholinos targeting the 5′ UTR region from –69 to –45 and the ATG region from –2 to +23 were synthesized from Gene Tools (Philomath, OR, USA), respectively. In addition, a mismatch morpholino was used as a control. To confirm the effectiveness of the zDDX11 morpholinos, a DNA fragment containing the morpholino target regions and the coding sequence of EGFP was generated using PCR and sub-cloned in frame into the pCS2+ plasmid. At the single-cell stage, zebrafish embryos were injected with zDDX11-specific or control morpholinos in combination with pCS2+ plasmids at doses of 6 ng morpholino and 100 ng pCS2+ plasmids. Fluorescence was detected and imaged using a fluorescent microscope (Zeiss, Oberknochen, Germany).

The morpholinos were injected into single-cell stage zebrafish embryos at doses of 6, 9 and 12 ng/embryo. Uninjected and injected embryos were then incubated under standard conditions for 24 h to assess their viability. Morphological differences among the zebrafish injected with either zDDX11-specific or control morpholinos were assessed under an Olympus SZX12 stereoscope at 3, 5 and 7 days post-injection (d.p.i.).

References

1. Lohman, T.M. and Bjornson, K.P. (1996) Mechanisms of helicase-catalyzed DNA unwinding. *Annu. Rev. Biochem.*, **65**, 169–214.
2. Singleton, M.R., Dillingham, M.S. and Wigley, D.B. (2007) Structure and mechanism of helicases and nucleic acid translocases. *Annu. Rev. Biochem.*, **76**, 23–50.
3. Cordin, O., Banroques, J., Tanner, N.K. and Linder, P. (2006) The DEAD-box protein family of RNA helicases. *Gene*, **367**, 17–37.
4. Linder, P. (2006) Dead-box proteins: a family affair–active and passive players in RNP-remodeling. *Nucleic Acids Res.*, **34**, 4168–4180.
5. Jarmoskaite, I. and Russell, R. (2011) DEAD-box proteins as RNA helicases and chaperones. *Wiley Interdiscip. Rev. RNA*, **2**, 135–152.
6. Kralund, H.H., Ousager, L., Jaspers, N.G., Raams, A., Pedersen, E.B., Gade, E. and Bygum, A. (2013) Xeroderma pigmentosum–trichothiodystrophy overlap patient with novel XPD/ERCC2 mutation. *Rare Dis.*, **1**, e24932.
7. Guo, M., Vidhyasagar, V., Ding, H. and Wu, Y. (2014) Insight into the roles of helicase motif Ia by characterizing Fanconi anemia group J protein (FANCJ) patient mutations. *J. Biol. Chem.*, **289**, 10551–10565.
8. van der Lelij, P., Chrzanowska, K.H., Godthelp, B.C., Rooi-mans, M.A., Oostra, A.B., Stumm, M., Zdzienicka, M.Z., Joenje, H. and de Winter, J.P. (2010) Warsaw breakage syndrome, a co-hesinopathy associated with mutations in the XPD helicase family member DDX11/ChlR1. *Am. J. Hum. Genet.*, **86**, 262–266.
9. Capo-Chichi, J.M., Bharti, S.K., Sommers, J.A., Yammine, T., Chouery, E., Patry, L., Rouleau, G.A., Samuels, M.E., Hamdan, F.F., Michaud, J.L. *et al.* (2013) Identification and biochemical characterization of a novel mutation in DDX11 causing Warsaw breakage syndrome. *Hum. Mutat.*, **34**, 103–107.
10. Wu, Y., Sommers, J.A., Khan, I., de Winter, J.P. and Brosh, R. M. Jr. (2012) Biochemical characterization of Warsaw breakage syndrome helicase. *J. Biol. Chem.*, **287**, 1007–1021.
11. Gerring, S.L., Spencer, F. and Hieter, P. (1990) The CHL 1 (CTF 1) gene product of Saccharomyces cerevisiae is important for chromosome transmission and normal cell cycle progression in G2/M. *EMBO J.*, **9**, 4347–4358.
12. Holloway, S.L. (2000) CHL1 is a nuclear protein with an essential ATP binding site that exhibits a size-dependent effect on chromosome segregation. *Nucleic Acids Res.*, **28**, 3056–3064.
13. Parish, J.L., Rosa, J., Wang, X., Lahti, J.M., Doxsey, S.J. and An-drophy, E.J. (2006) The DNA helicase ChlR1 is required for sister chromatid cohesion in mammalian cells. *J. Cell Sci.*, **119**, 4857–4865.

14. Inoue, A., Li, T., Roby, S.K., Valentine, M.B., Inoue, M., Boyd, K., Kidd, V.J. and Lahti, J.M. (2007) Loss of ChlR1 helicase in mouse causes lethality due to the accumulation of aneuploid cells generated by cohesion defects and placental malformation. *Cell Cycle*, **6**, 1646–1654.

15. Farina, A., Shin, J.H., Kim, D.H., Bermudez, V.P., Kelman, Z., Seo, Y.S. and Hurwitz, J. (2008) Studies with the human cohesin establishment factor, ChlR1. Association of ChlR1 with Ctf18-RFC and Fen1. *J. Biol. Chem.*, **283**, 20925–20936.

16. Wu, Y. and Brosh, R.M. Jr. (2012) DNA helicase and helicase-nuclease enzymes with a conserved iron-sulfur cluster. *Nucleic Acids Res.*, **40**, 4247–4260.

17. Rudra, S. and Skibbens, R.V. (2013) Chl1 DNA helicase regulates Scc2 deposition specifically during DNA-replication in *Saccharomyces cerevisiae*. *PLoS ONE*, **8**, e75435.

18. Shah, N., Inoue, A., Woo Lee, S., Beishline, K., Lahti, J.M. and Noguchi, E. (2013) Roles of ChlR1 DNA helicase in replication recovery from DNA damage. *Exp. Cell Res.*, **319**, 2244–2253.

19. Cota, C.D. and Garcia-Garcia, M.J. (2012) The ENU-induced cetus mutation reveals an essential role of the DNA helicase DDX11 for mesoderm development during early mouse embryogenesis. *Dev. Dyn.*, **241**, 1249–1259.

20. McLeod, T., Abdullahi, A., Li, M. and Brogna, S. (2014) Recent studies implicate the nucleolus as the major site of nuclear translation. *Biochem. Soc. Trans.*, **42**, 1224–1228.

21. Panov, K.I., Friedrich, J.K. and Zomerdijk, J.C. (2001) A step subsequent to preinitiation complex assembly at the ribosomal RNA gene promoter is rate limiting for human RNA polymerase I-dependent transcription. *Mol. Cell Biol.*, **21**, 2641–2649.

22. Sanij, E. and Hannan, R.D. (2009) The role of UBF in regulating the structure and dynamics of transcriptionally active rDNA chromatin. *Epigenetics*, **4**, 374–382.

23. Santoro, R., Schmitz, K.M., Sandoval, J. and Grummt, I. (2010) Intergenic transcripts originating from a subclass of ribosomal DNA repeats silence ribosomal RNA genes in trans. *EMBO Rep.*, **11**, 52–58.

24. Nosrati, N., Kapoor, N.R. and Kumar, V. (2014) Combinatorial action of transcription factors orchestrates cell cycle-dependent expression of the ribosomal protein genes and ribosome biogenesis. *FEBS J.*, **281**, 2339–2352.

25. McStay, B. and Grummt, I. (2008) The epigenetics of rRNA genes: from molecular to chromosome biology. *Annu. Rev. Cell Dev. Biol.*, **24**, 131–157.

26. Pietrzak, M., Rempala, G., Nelson, P.T., Zheng, J.J. and Hetman, M. (2011) Epigenetic silencing of nucleolar rRNA genes in Alzheimer's disease. *PLoS ONE*, **6**, e22585.

27. Zentner, G.E., Hurd, E.A., Schnetz, M.P., Handoko, L., Wang, C., Wang, Z., Wei, C., Tesar, P.J., Hatzoglou, M., Martin, D.M. *et al.* (2010) CHD7 functions in the nucleolus as a positive regulator of ribosomal RNA biogenesis. *Hum. Mol. Genet.*, **19**, 3491–3501.

28. Sheng, J., Yu, W., Gao, X., Xu, Z. and Hu, G.F. (2014) Angiogenin stimulates ribosomal RNA transcription by epigenetic activation of the ribosomal DNA promoter. *J. Cell. Physiol.*, **229**, 521–529.

29. Zhu, Z., Wang, Y., Li, X., Xu, L., Wang, X., Sun, T., Dong, X., Chen, L., Mao, H., Yu, Y. *et al.* (2010) PHF8 is a histone H3K9me2 demethylase regulating rRNA synthesis. *Cell Res.*, **20**, 794–801.

30. Voit, R. and Grummt, I. (2001) Phosphorylation of UBF at serine 388 is required for interaction with RNA polymerase I and activation of rDNA transcription. *Proc. Natl Acad. Sci. USA*, **98**, 13631–13636.

31. Meraner, J., Lechner, M., Loidl, A., Goralik-Schramel, M., Voit, R., Grummt, I. and Loidl, P. (2006) Acetylation of UBF changes during the cell cycle and regulates the interaction of UBF with RNA polymerase I. *Nucleic Acids Res.*, **34**, 1798–1806.

32. Freed, E.F., Bleichert, F., Dutca, L.M. and Baserga, S.J. (2010) When ribosomes go bad: diseases of ribosome biogenesis. *Mol. Biosyst.*, **6**, 481–493.

33. Narla, A. and Ebert, B.L. (2010) Ribosomopathies: human disorders of ribosome dysfunction. *Blood*, **115**, 3196–3205.

34. Hannan, K.M., Sanij, E., Rothblum, L.I., Hannan, R.D. and Pearson, R.B. (2013) Dysregulation of RNA polymerase I transcription during disease. *Biochim. Biophys. Acta*, **1829**, 342–360.

35. Donati, G., Montanaro, L. and Derenzini, M. (2012) Ribosome biogenesis and control of cell proliferation: p53 is not alone. *Cancer Res.*, **72**, 1602–1607.

36. Russell, J. and Zomerdijk, J.C. (2005) RNA-polymerase-I-directed rDNA transcription, life and works. *Trends Biochem. Sci.*, **30**, 87–96.

37. Zhang, Y., Forys, J.T., Miceli, A.P., Gwinn, A.S. and Weber, J.D. (2011) Identification of DHX33 as a mediator of rRNA synthesis and cell growth. *Mol. Cell Biol.*, **31**, 4676–4691.

38. Kimura, H. (2013) Histone modifications for human epigenome analysis. *J. Hum. Genet.*, **58**, 439–445.

39. Klein, J. and Grummt, I. (1999) Cell cycle-dependent regulation of RNA polymerase I transcription: the nucleolar transcription factor UBF is inactive in mitosis and early G1. *Proc. Natl Acad. Sci. USA*, **96**, 6096–6101.

40. Meraner, J., Lechner, M., Schwarze, F., Gander, R., Jesacher, F. and Loidl, P. (2008) Cell cycle dependent role of HDAC1 for proliferation control through modulating ribosomal DNA transcription. *Cell Biol. Int.*, **32**, 1073–1080.

41. Tuan, J.C., Zhai, W. and Comai, L. (1999) Recruitment of TATA-binding protein-TAFI complex SL1 to the human ribosomal DNA promoter is mediated by the carboxy-terminal activation domain of upstream binding factor (UBF) and is regulated by UBF phosphorylation. *Mol. Cell Biol.*, **9**, 2872–2879.

42. Halkidou, K., Logan, I.R., Cook, S., Neal, D.E. and Robson, C.N. (2004) Putative involvement of the histone acetyltransferase Tip60 in ribosomal gene transcription. *Nucleic Acids Res.*, **32**, 1654–1665.

43. Panova, T.B., Panov, K.I., Russell, J. and Zomerdijk, J.C. (2006) Casein kinase 2 associates with initiation-competent RNA polymerase I and has multiple roles in ribosomal DNA transcription. *Mol. Cell Biol.*, **26**, 5957–5968.

44. Lee, J., Hwang, Y.J., Boo, J.H., Han, D., Kwon, O.K., Todorova, K., Kowall, N.W., Kim, Y. and Ryu, H. (2011) Dysregulation of upstream binding factor-1 acetylation at K352 is linked to impaired ribosomal DNA transcription in Huntington's disease. *Cell Death Differ.*, **18**, 1726–1735.

45. Tsai, R.Y. and Pederson, T. (2014) Connecting the nucleolus to the cell cycle and human disease. *FASEB J.*, **28**, 3290–3296.

46. Harris, B., Bose, T., Lee, K.K., Wang, F., Lu, S., Ross, R.T., Zhang, Y., French, S.L., Beyer, A.L., Slaughter, B.D. *et al.* (2014) Cohesion promotes nucleolar structure and function. *Mol. Biol. Cell*, **25**, 337–346.

47. Vaitiekunaite, R., Butkiewicz, D., Krzesniak, M., Przybylek, M., Gryc, A., Snietura, M., Benedyk, M., Harris, C.C. and Rusin, M. (2007) Expression and localization of Werner syndrome protein is modulated by SIRT1 and PML. *Mech. Ageing Dev.*, **128**, 650–661.

48. Wang, J., Leung, J.W., Gong, Z., Feng, L., Shi, X. and Chen, J. (2013) PHF6 regulates cell cycle progression by suppressing ribosomal RNA synthesis. *J. Biol. Chem.*, **288**, 3174–3183.

49. Ganapathi, K.A., Austin, K.M., Lee, C.S., Dias, A., Malsch, M.M., Reed, R. and Shimamura, A. (2007) The human Shwachman–

Diamond syndrome protein, SBDS, associates with ribosomal RNA. *Blood*, **110**, 1458–1465.

50. Sondalle, S.B. and Baserga, S.J. (2014) Human diseases of the SSU processome. *Biochim. Biophys. Acta*, **1842**, 758–764.

51. Alazami, A.M., Al-Saif, A., Al-Semari, A., Bohlega, S., Zlitni, S., Alzahrani, F., Bavi, P., Kaya, N., Colak, D., Khalak, H. *et al.* (2008) Mutations in C2orf37, encoding a nucleolar protein, cause hypogonadism, alopecia, diabetes mellitus, mental retardation, and extrapyramidal syndrome. *Am. J. Hum. Genet.*, **83**, 684–691.

52. Abidi, F., Miano, M., Murray, J. and Schwartz, C. (2007) A novel mutation in the PHF8 gene is associated with X-linked mental retardation with cleft lip/cleft palate. *Clin. Genet.*, **72**, 19–22.

53. Loenarz, C., Ge, W., Coleman, M.L., Rose, N.R., Cooper, C.D., Klose, R.J., Ratcliffe, P.J. and Schofield, C.J. (2010) PHF8, a gene associated with cleft lip/palate and mental retardation, encodes for an Nepsilon-dimethyl lysine demethylase. *Hum. Mol. Genet.*, **19**, 217–222.

54. Feng, W., Yonezawa, M., Ye, J., Jenuwein, T. and Grummt, I. (2010) PHF8 activates transcription of rRNA genes through H3K4me3 binding and H3K9me1/2 demethylation. *Nat. Struct. Mol. Biol.*, **17**, 445–450.

55. Abdelhaleem, M., Maltais, L. and Wain, H. (2003) The human DDX and DHX gene families of putative RNA helicases. *Genomics*, **81**, 618–622.

56. Jain, A., Bacolla, A., Chakraborty, P., Grosse, F. and Vasquez, K. M. (2010) Human DHX9 helicase unwinds triple-helical DNA structures. *Biochemistry*, **49**, 6992–6999.

57. van der Lelij, P., Oostra, A.B., Rooimans, M.A., Joenje, H. and de Winter, J.P. (2010) Diagnostic overlap between fanconi anemia and the cohesinopathies: Roberts syndrome and Warsaw breakage syndrome. *Anemia*, **2010**, 565268.

58. Lu, S., Lee, K.K., Harris, B., Xiong, B., Bose, T., Saraf, A., Hattem, G., Florens, L., Seidel, C. and Gerton, J.L. (2014) The cohesin acetyltransferase Eco1 coordinates rDNA replication and transcription. *EMBO Rep.*, **15**, 609–617.

59. Xu, B., Lu, S. and Gerton, J.L. (2014) Roberts syndrome: A deficit in acetylated cohesin leads to nucleolar dysfunction. *Rare Dis.*, **2**, e27743.

60. Ma, Z., Kanai, M., Kawamura, K., Kaibuchi, K., Ye, K. and Fukasawa, K. (2006) Interaction between ROCK II and nucleophosmin/B23 in the regulation of centrosome duplication. *Mol. Cell Biol.*, **26**, 9016–9034.

61. Ugrinova, I., Monier, K., Ivaldi, C., Thiry, M., Storck, S., Mongelard, F. and Bouvet, P. (2007) Inactivation of nucleolin leads to nucleolar disruption, cell cycle arrest and defects in centrosome duplication. *BMC Mol. Biol.*, **8**, 66.

62. Chen, C.C., Greene, E., Bowers, S.R. and Mellone, B.G. (2012) A role for the CAL1-partner Modulo in centromere integrity and accurate chromosome segregation in *Drosophila*. *PLoS ONE*, **7**, e45094.

63. Amin, M.A., Matsunaga, S., Uchiyama, S. and Fukui, K. (2008) Nucleophosmin is required for chromosome congression, proper mitotic spindle formation, and kinetochore-microtubule attachment in HeLa cells. *FEBS Lett.*, **582**, 3839–3844.

64. Rabitsch, K.P., Petronczki, M., Javerzat, J.P., Genier, S., Chwalla, B., Schleiffer, A., Tanaka, T.U. and Nasmyth, K. (2003) Kinetochore recruitment of two nucleolar proteins is required for homolog segregation in meiosis I. *Dev. Cell*, **4**, 535–548.

65. Sihn, C.R., Lee, Y.S., Jeong, J.S., Park, K. and Kim, S.H. (2008) CANu1, a novel nucleolar protein, accumulated on centromere in response to DNA damage. *Genes Cells*, **13**, 787–796.

66. Varela, E., Schlecht, U., Moina, A., Fackenthal, J.D., Washburn, B.K., Niederhauser-Wiederkehr, C., Tsai-Pflugfelder, M., Primig, M., Gasser, S.M. and Esposito, R.E. (2010) Mitotic expression of Spo13 alters M-phase progression and nucleolar localization of Cdc14 in budding yeast. *Genetics*, **185**, 841–854.

67. Yuan, L., Yang, X., Auman, D. and Makaroff, C.A. (2014) Expression of epitope-tagged SYN3 cohesin proteins can disrupt meiosis in Arabidopsis. *J. Genet. Genomics*, **41**, 153–164.

68. Pluta, A.F. and Earnshaw, W.C. (1996) Specific interaction between human kinetochore protein CENP-C and a nucleolar transcriptional regulator. *J. Biol. Chem.*, **271**, 18767–18774.

69. Wong, L.H., Brettingham-Moore, K.H., Chan, L., Quach, J.M., Anderson, M.A., Northrop, E.L., Hannan, R., Saffery, R., Shaw, M.L., Williams, E. and Choo, K.H. (2007) Centromere RNA is a key component for the assembly of nucleoproteins at the nucleolus and centromere. *Genome Res.*, **17**, 1146–1160.

70. Peng, Q., Wu, J., Zhang, Y., Liu, Y., Kong, R., Hu, L., Du, X. and Ke, Y. (2010) 1A6/DRIM, a novel t-UTP, activates RNA polymerase I transcription and promotes cell proliferation. *PLoS ONE*, **5**, e14244.

71. Ghoshal, K., Majumder, S., Datta, J., Motiwala, T., Bai, S., Sharma, S.M., Frankel, W. and Jacob, S.T. (2004) Role of human ribosomal RNA (rRNA) promoter methylation and of methyl-CpG-binding protein MBD2 in the suppression of rRNA gene expression. *J. Biol. Chem.*, **279**, 6783–6793.

72. Andersen, J.S., Lyon, C.E., Fox, A.H., Leung, A.K., Lam, Y.W., Steen, H., Mann, M. and Lamond, A.I. (2002) Directed proteomic analysis of the human nucleolus. *Curr. Biol.*, **12**, 1–11.

73. Grandori, C., Gomez-Roman, N., Felton-Edkins, Z.A., Ngouenet, C., Galloway, D.A., Eisenman, R.N. and White, R.J. (2005) c-Myc binds to human ribosomal DNA and stimulates transcription of rRNA genes by RNA polymerase I. *Nat. Cell Biol.*, **7**, 311–318.

74. Azuma, M., Toyama, R., Laver, E. and Dawid, I.B. (2006) Perturbation of rRNA synthesis in the bap28 mutation leads to apoptosis mediated by p53 in the zebrafish central nervous system. *J. Biol. Chem.*, **281**, 13309–13316.

75. He, W., Zhao, Y., Zhang, C., An, L., Hu, Z., Liu, Y., Han, L., Bi, L., Xie, Z., Xue, P. *et al.* (2008) Rad9 plays an important role in DNA mismatch repair through physical interaction with MLH1. *Nucleic Acids Res.*, **36**, 6406–6417.

76. He, W., Ma, X., Yang, X., Zhao, Y., Qiu, J. and Hang, H. (2011) A role for the arginine methylation of Rad9 in checkpoint control and cellular sensitivity to DNA damage. *Nucleic Acids Res.*, **39**, 4719–4727.

77. Nelson, J.D., Denisenko, O. and Bomsztyk, K. (2006) Protocol for the fast chromatin immunoprecipitation (ChIP) method. *Nat. Protoc.*, **1**, 179–185.

78. O'Sullivan, A.C., Sullivan, G.J. and McStay, B. (2002) UBF binding in vivo is not restricted to regulatory sequences within the vertebrate ribosomal DNA repeat. *Mol. Cell Biol.*, **22**, 657–668.